

Radiation-Field-Dependent Frequency Shifts of Atomic Beam Resonances

ROBERT J. HARRACH*

National Bureau of Standards, Boulder, Colorado

(Received 21 July 1966; in final form 14 November 1966)

Radiation-field-dependent frequency shifts arising in atomic-beam spectroscopy are treated theoretically and experimentally. Shifts due to fundamental and unavoidable interactions between the radiation field and the atoms comprising the beam are distinguished from those due to various "apparatus effects." Precise measurements of frequency shifts are made for a cesium beam experiencing Ramsey-type excitation. For the magnetic-field-sensitive transitions $(F, M_F) = (4, \pm 1) \leftrightarrow (3, \pm 1)$, the magnitude of the shifts is about 1 part in 10^{10} of the resonance frequency value, per milliwatt variation of input power to the radiation field. The shifts vary with input intensity in a nonmonotonic fashion and are shown to result from nonuniformity in the static magnetic c -field of the apparatus. Much smaller shifts of about 5 parts in 10^{13} per milliwatt are observed for the magnetic-field-insensitive transition $(F, M_F) = (4, 0) \leftrightarrow (3, 0)$. The major features of these shifts are shown to arise from spectral impurities in the radiation exciting the transition and a small phase difference between the pair of separated radiation fields. The bearing these results have on evaluating the accuracy of an atomic beam frequency standard is discussed.

I. INTRODUCTION

THE resonance frequencies measured in atomic beam spectroscopy are usually presumed to be the Bohr frequencies corresponding to stationary-state energy level separations of atoms in the beam. This is not exactly the case, however, and a large class of resonance frequency shifts (departures from the Bohr values) depend on the intensity of the radiation field used to excite a transition. This paper is a theoretical and experimental study of these radiation-field-dependent, or "power"-dependent, frequency shifts as they arise in an atomic beam experiment of the Ramsey type, employing excitation by a pair of separated radiation fields.

Factors causing shifts fall conveniently into two categories. Those of a fundamental character stem from the unavoidable features of the motion of atoms

(Doppler effect), the structure of atoms (effect of neighboring energy levels), and the properties of the transition-inducing radiation field (Bloch-Siegert and Stark effects). Other factors are not fundamental, but are present because the atomic beam apparatus falls short of ideality. For example, the static magnetic c -field is not precisely uniform, the phases of the pair of radiation fields are not quite equal, and the radiation fields are not truly monochromatic.

The theoretical discussion of apparatus effects begins in Sec. II. The derivations are based on computer-analyzed line shapes, using the full Maxwellian velocity distribution of atoms in the beam. In Sec. III, the velocity-averaged results for shifts due to the fundamental factors are discussed.

The experimental results are taken up in Sec. IV, where frequency shifts of the magnetic-field-sensitive transitions $(F, M_F) = (4, \pm 1) \leftrightarrow (3, \pm 1)$ in cesium are described. These are nonmonotonic, with a magnitude of about 1 part in 10^{10} of the resonance frequency

* Present address: Lawrence Radiation Laboratory, University of California, Livermore.

value, per milliwatt variation of input intensity to the radiation fields. It is shown that these shifts are generated by c -field nonuniformity. Then the much smaller shift (about 5 parts in 10^{13} per milliwatt) of the magnetic-field-insensitive transition $(F, M_F) = (4, 0) \leftrightarrow (3, 0)$ in cesium is analyzed. This transition provides the definition for the United States frequency standard. The extent to which the various shift factors can be evaluated and corrections made for them determines the limit of accuracy of the standard. Emphasized is the importance in evaluating the limits of accuracy of measuring the radiation-field dependence of the resonance, in conjunction with supplementary experiments, such as reversing the beam direction through the apparatus, varying the c -field magnitude, and varying the spectrum of the radiation-inducing transitions.

II. THEORY OF APPARATUS EFFECTS

The usual formulation of the atomic-beam problem utilizes the "two-level" and "rotating field" approxi-

mations: An atom in the presence of a weak static magnetic field, \mathbf{H}_c , is assumed to have only two stationary state energy levels, say, W_p and W_q , with corresponding eigenfunctions, $u_p(\mathbf{x})$ and $u_q(\mathbf{x})$. The Bohr separation frequency of the levels is then $\nu_0 = (W_q - W_p)/h$. The oscillating radiation field which induces transitions is assumed to have the time dependence $\exp(i\omega t)$, rather than $\sin(\omega t)$. Most of the apparatus effects leading to frequency shifts can be described within the framework of these approximations.

A method of calculating the transition probability for an atom initially in a state p to be found in a state q after traversing a pair of rotating fields separated by a "drift" region has been described by Ramsey.¹ If we treat the case where the phase of the second radiation field leads that of the first by an amount δ , and the amplitudes of the first and second fields are $H_r(1)$ and $H_r(2)$, respectively, then the approximate (near resonance) transition probability, averaged over the usual Maxwellian velocity distribution¹ of atoms, is calculated to be

$$\begin{aligned} \langle P_{pq} \rangle = & \frac{1}{4} [U_0(\phi_1, \phi_2) + \cos(\delta) U_1(\phi_1, \phi_2, \theta) + \sin(\delta) W_1(\phi_1, \phi_2, \theta)] \\ & + (\Delta/8) [(1/\phi_2) + (1/\phi_1)] [\cos(\delta) U_2(\phi_1, \phi_2, \theta) + \sin(\delta) W_2(\phi_1, \phi_2, \theta)] \\ & + (\Delta/8) [(1/\phi_2) - (1/\phi_1)] [\cos(\delta) U_3(\phi_1, \phi_2, \theta) + \sin(\delta) W_3(\phi_1, \phi_2, \theta)]. \quad (\text{II.1}) \end{aligned}$$

In this expression, the angular frequency, ω , of the radiation field is specified by

$$\theta = (\bar{\omega}_0 - \omega) L / \alpha, \quad (\text{II.2})$$

and the radiation field amplitudes are given by

$$\phi_k = 4b_k l / \alpha, \quad k = 1, 2, \quad (\text{II.3})$$

with

$$2b_k = \frac{-1}{\hbar} \int u_p^*(\mathbf{x}) \mathbf{u} \cdot \mathbf{H}_r(k) u_q(\mathbf{x}) d\mathbf{x}, \quad (\text{II.4})$$

where \mathbf{u} is the magnetic dipole moment of the atom. The quantities l , L , α , and $\bar{\omega}_0$ are the same as used by Ramsey. The U -functions are

$$\begin{aligned} U_0(\phi_1, \phi_2) &= 2 - 2I[(\phi_1 + \phi_2)/2] - 2I[(\phi_1 - \phi_2)/2], \\ U_1(\phi_1, \phi_2, \theta) &= I[\theta + (\phi_1 - \phi_2)/2] + I[\theta - (\phi_1 - \phi_2)/2] - I[\theta + (\phi_1 + \phi_2)/2] - I[\theta - (\phi_1 + \phi_2)/2], \\ U_2(\phi_1, \phi_2, \theta) &= I[\theta - (\phi_1 + \phi_2)/2] - I[\theta + (\phi_1 + \phi_2)/2] + I[\theta + \phi_2/2] - I[\theta - \phi_2/2] + I[\theta + \phi_1/2] - I[\theta - \phi_1/2], \\ U_3(\phi_1, \phi_2, \theta) &= I[\theta - (\phi_1 - \phi_2)/2] - I[\theta + (\phi_1 - \phi_2)/2] + I[\theta - \phi_2/2] - I[\theta + \phi_2/2] + I[\theta + \phi_1/2] - I[\theta - \phi_1/2]. \quad (\text{II.5}) \end{aligned}$$

The functions W_k , $k = 1, 2, 3$, are identical to the functions U_k , $k = 1, 2, 3$, respectively, except that each $I(\chi)$ appearing in the U 's is replaced by $K(\chi)$. The $I(\chi)$ and $K(\chi)$ are numerically tabulated integrals:²

$$\begin{aligned} I(\chi) &= \int_0^\infty y^3 \exp(-y^2) \cos(\chi/y) dy, \\ K(\chi) &= \int_0^\infty y^3 \exp(-y^2) \sin(\chi/y) dy. \quad (\text{II.6}) \end{aligned}$$

An important measure of c -field nonuniformity is given by the quantity Δ , which is

$$\Delta = 4l(\omega_0 - \bar{\omega}_0) / \alpha. \quad (\text{II.7})$$

The average c -field magnitude in the transition regions determines the Bohr frequency ω_0 , and the average c -field magnitude in the drift region determines $\bar{\omega}_0$. For a nonuniform c -field, these quantities will not be in general, equal.

The ideal apparatus case¹ is obtained by setting

¹N. Ramsey, *Molecular Beams* (Oxford University Press, New York, 1956).

²A tabulation of the integrals is given in Appendix D of the reference of footnote 1. For the analysis of this paper a more detailed tabulation provided by Dr. J. Shirley was used, including a range of arguments $0 \leq \chi \leq 10$, with χ varying in increments of 0.02.

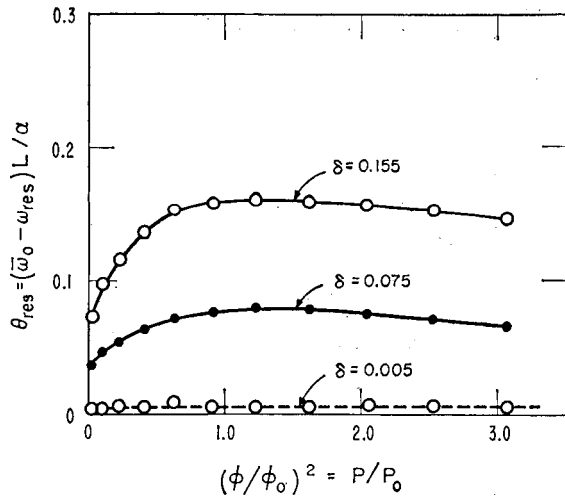


FIG. 1. Theoretical frequency shift induced by a small phase difference, δ (radians), as a function of excitation intensity.

$\phi_1 = \phi_2 = \phi$, $\Delta = 0$, and $\delta = 0$. The value of θ which maximizes the transition probability for any radiation field magnitude, given by ϕ , is $\theta_{\text{res}} = (\bar{\omega}_0 - \omega_{\text{res}})L/\alpha = 0$. Thus, the resonance frequency is exactly the drift region average Bohr frequency, independent of radiation field intensity. The optimum ϕ -value, which gives the maximum transition probability at resonance, is

$$\phi_0 = 4b_0l/\alpha = (1.20)\pi. \quad (\text{II.8})$$

An ideal apparatus can be closely approximated in practice, but one can expect the presence of small phase and amplitude differences between the radiation fields, and some degree of c -field nonuniformity which gives the factor Δ , which we will call the " c -field difference factor," a finite value. The effect on the resonance frequency of each of these features will be considered, first in isolation, then when they act in concert.

A phase difference between the radiation fields is minimized by using a single U-shaped cavity with the beam passing through its ends. But because of small faults of cavity construction, stresses, contamination, and slight nonuniformities in the loss properties of the cavity walls, some finite phase difference remains. Its value, as "averaged" by the beam, may be only of the order 10^{-3} rad, but even then gives rise to observable effects. In Fig. 1, the power-dependent frequency shifts caused by phase differences of several different magnitudes are shown, where it is assumed that the rf amplitudes are equal and the c -field difference factor is zero. The abscissa of the figure is $(\phi/\phi_0)^2$, and since ϕ is proportional to the radiation field magnitude, and ϕ_0 to the optimum magnitude, this quantity equals the ratio of experimental input power, P , to the optimum input power, P_0 . From Fig. 1, we conclude that the resonance frequency at optimum intensity is given in terms of a small phase difference, $\delta \ll 2\pi$, by

$$\omega_{\text{res}} - \bar{\omega}_0 \cong -(1.0)\alpha\delta/L, \quad (\text{II.9})$$

and that the amount of shift is not very sensitive to the level of radiation field intensity. When the beam direction through the apparatus is reversed, the sign of δ changes, and the net frequency difference for the two beam directions (at optimum intensity) is $\Delta\nu = \Delta\omega/2\pi \cong \alpha\delta/\pi L$. This procedure of reversing the beam direction, which has long been a practice in some laboratories, enables the effect of δ to be eliminated, and, using the relation for $\Delta\nu$, the phase difference can be evaluated. However, care must be taken to assure that only the sign of δ , and not its magnitude, is altered in the reversal process. This point will be elaborated in Sec. IV.

We have noted that c -field nonuniformity, which results from imperfections in the magnetic shielding and c -field geometry, can make the average c -field magnitude in the drift region, $\bar{H}_c(L)$, differ from the average value in the transition regions, $\bar{H}_c(l)$. (We assume that the c -field magnitudes in the two transition regions are equal, with no important loss of generality.) For magnetic-field-sensitive transitions, the Bohr frequencies vary linearly with field in lowest order, and Δ can easily have a magnitude of order unity. Using these transitions, the quantity $(\omega_0 - \bar{\omega}_0)$ can be experimentally evaluated from calibrated line shape traces, by noting that the central Ramsey peak lies very nearly at $\bar{\omega}_0$, while the broad resonance pedestal is centered at ω_0 .¹ On the other hand, transitions which qualify as frequency standards are magnetic-field-insensitive, depending quadratically on field in lowest order. For these, Δ has a much smaller magnitude.

The radiation-field-dependent frequency shifts for

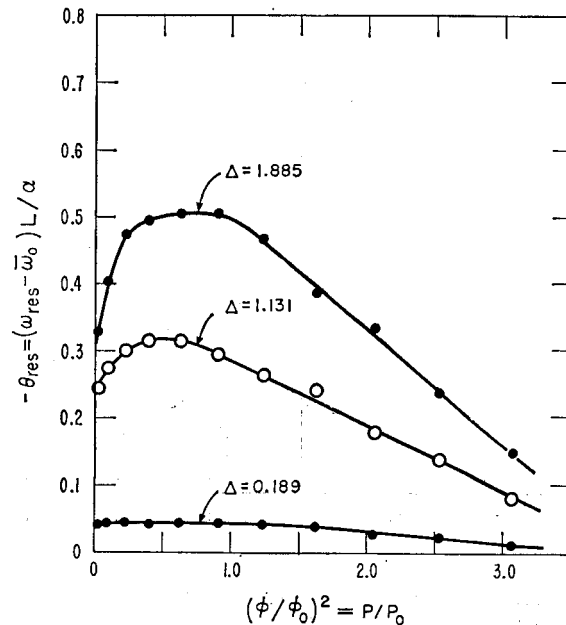


FIG. 2. Theoretical frequency shift induced by the dy c -field difference factor, $\Delta = 4l(\omega_0 - \bar{\omega}_0)/\alpha$, as a function of excitation intensity.

various Δ -values are shown in Fig. 2. At optimum intensity, it is seen that $\theta_{\text{res}} = (\bar{\omega}_0 - \omega_{\text{res}})L/\alpha \cong -(0.25)\Delta$, or, using Eq. (II.7),

$$\omega_{\text{res}} - \bar{\omega}_0 \cong + (1.0)l(\omega_0 - \bar{\omega}_0)/L. \quad (\text{II.10})$$

For sizable Δ -factors, the variation of the resonance frequency with intensity shows a "turn-over" point, where the shift direction reverses. We can express this power-dependence symbolically by

$$\omega_{\text{res}} = \bar{\omega}_0 + k(P)l(\omega_0 - \bar{\omega}_0)/L, \quad (\text{II.11})$$

where $k(P)$ exhibits the nonmonotonic behavior given in Fig. 2. For example, $k(P)$ might rise with increasing power, then begin a slope reversal at some "critical" power level, then fall with further increase in power. At optimum power, $k(P_0) \cong 1.0$, and in the limit of very high power, $k(P)$ approaches zero.

The radiation field mode commonly used in atomic beam machines is a $\text{TE}_{1,0,n}$ mode, in which the important magnetic component has constant magnitude along the length of the transition region, but varies in magnitude over the height of the beam (along the z coordinate, say) as $H_{r_0} \cos(2\pi z/\lambda_0)$. Most atoms will not have exactly the same z coordinate in the two transition regions, and therefore will experience excitation by radiation fields at different amplitudes. This effect, like the phase difference, is averaged by the beam, and the resulting amplitude difference which characterizes the beam as a whole will be small compared to the largest difference value possible for a single atom. If the beam is perfectly aligned, the net amplitude difference value is zero.

It is easily seen that an amplitude difference will cause no frequency shift when acting in isolation.

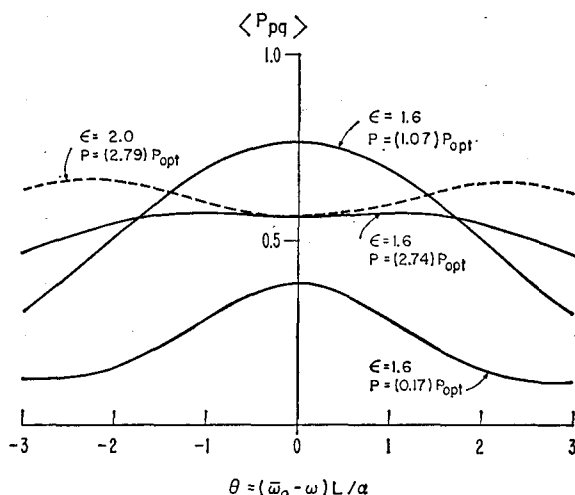


FIG. 3. Some near resonance line shapes for the case of excitation by unequal rf amplitudes. The amplitude of the first (second) radiation field is ϵH_r , and that of the second (first) field is H_r . The optimum power is determined using the equations $\phi_{\text{opt}} = \phi_0/\frac{1}{2}(1+\epsilon)$ [see Eqs. (II.8) and (II.12) in text] and $(\phi/\phi_{\text{opt}})^2 = P/P_{\text{opt}}$.

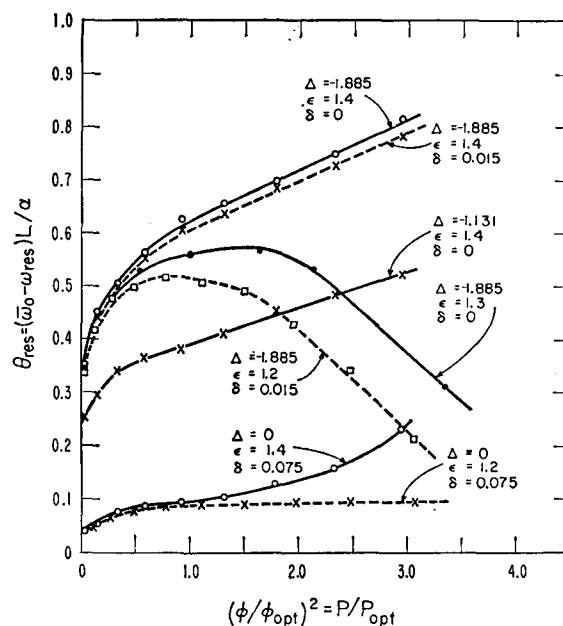


FIG. 4. Theoretical frequency shifts induced by a small phase difference, δ (radians), and a c -field difference factor, $\Delta = 4l(\omega_0 - \bar{\omega}_0)/\alpha$, in the presence of excitation by unequal rf amplitudes ($\epsilon H_r, H_r$).

When $\delta = 0 = \Delta$, but $\phi_1 \neq \phi_2$, the transition probability (II.1) is symmetrical in θ , so that the center of symmetry of the resonance line is always at $\theta = 0$, or $\omega_{\text{res}} = \bar{\omega}_0$. Several near resonance line shapes for this case are shown in Fig. 3. When the ϕ -factors for the two transition regions are $\phi_1 = m\phi$ and $\phi_2 = m'\phi$, the optimum ϕ -value is

$$\phi_{\text{opt}} = \phi_0/\frac{1}{2}(m+m'), \quad (\text{II.12})$$

with ϕ_0 given by (II.8). Thus $\phi_1 + \phi_2 = 2\phi_0$ is an invariant optimum amplitude condition. It is seen from the figure that at excessive excitation intensities, the center of symmetry of the resonance line may become a minimum instead of a maximum.³

What is most relevant to our discussion is the manner in which a net amplitude difference enhances frequency shifts due to phase difference and c -field nonuniformity. This is shown in Fig. 4. Most notably, the turn-over point of the Δ -shift is delayed, to occur at a higher level of intensity, and the δ -shift is made to vary more strongly with radiation field intensity.

In addition to the apparatus effects just described, it is necessary to take into account several others. First, the spectrum of the transition-inducing radiation usually contains sidebands in addition to the primary component. If slight imbalances exist in the intensities of sideband pairs located symmetrically above and below the primary frequency, then a net pulling of the resonance occurs. This pulling has been calculated by

³ N. Ramsey, *Recent Research in Molecular Beams*, I. Estermann, Ed. (Academic Press, New York, 1959).

Ramsey³ for the case where the separation frequency of an unbalanced sideband from the primary is large relative to the matrix element for that sideband, i.e., $|\bar{\omega}_0 - \omega_i| \gg |2b_i|$. This approximation is adequate for our purposes, since interest will be in sidebands about 30 dB or more below the primary intensity, and removed by several tens of cps. As the excitation intensity is decreased toward very low values, as is done in the power-shift experiments to be described, this approximation becomes even better. Ramsey's procedure is to let the extraneous perturbation, with frequency ω_i and matrix element b_i , act over an effective length of $(1/2)l$ just after the first transition region and just before the second. The near resonance transition probability is then easily calculable, and, when averaged over the Maxwellian velocity distribution, the leading term gives

$$\langle P_{pq} \rangle = \frac{1}{4} [1 - 2I(\phi) + 2I(\theta') - I(\theta' + \phi) - I(\theta' - \phi)],$$

where

$$\theta' \cong \theta + l(2b_i)^2 / 2\alpha(\bar{\omega}_0 - \omega_i).$$

For any rf magnitude, given by $\phi = 4bl/\alpha$, the resonance occurs for $\theta' = 0$, or

$$\omega_{\text{res}} = \bar{\omega}_0 + l(2b_i)^2 / 2L(\bar{\omega}_0 - \omega_i). \quad (\text{II.13})$$

We can use the relations

$$(2b_i)^2 / (2b)^2 = P_{\text{sb}} / P = A_i, \quad (2b)^2 / (2b_0)^2 = P / P_0,$$

where A_i is then the ratio of sideband intensity to primary intensity, and P_0 is the experimental optimum primary intensity. Then the frequency shift is

$$\omega_{\text{res}} - \bar{\omega}_0 = lA_i(2b_0)^2 P / 2L(\bar{\omega}_0 - \omega_i) P_0, \quad (\text{II.14})$$

with b_0 given by (II.8). For an array of sidebands, the effect due to each is independent in this approximation, and the rhs of (II.14) is summed over i . The presence of these linear power shifts can be ascertained by intentionally altering the excitation spectrum.

This method of calculation may be applied to cases where the extraneous excitation is not actually present in the spectrum, but arises, e.g., because spatial variations in the c -field direction or the radiation field direction appear as effective rotating fields to the moving atoms.³ In this connection, it is worth noting that if the extraneous perturbation of a two-level quantum system occurs outside the transition and drift regions, i.e., before the first transition region and after the second, then the calculation predicts no frequency pulling. Also, it should be noted that the matrix element b_i for the extraneous field component satisfies magnetic dipole selection rules. In particular, if p and q are two states with the same M_F quantum number, then for an extraneous field which oscillates perpendicular to the static c field, $b_i = 0$.

Other apparatus effects that can be important are

physical overlap of neighboring resonances and cavity pulling. The frequency shift due to the former varies approximately inversely as the cube of the separation between neighboring resonances,⁴ and diminishes as the excitation intensity is reduced below the optimum value, since the resonance lines become narrower and weaker. The shift due to cavity pulling is proportional to the amount that the cavity is detuned.⁴ In the experiments to be described, both of these effects are negligibly small and will not be discussed further. Finally, various servo-system effects can lead to shifts of the resonance frequency. These require a detailed set of experiments for their analysis⁵ and will not be treated in this paper.

III. FUNDAMENTAL EFFECTS

The most familiar of the unavoidable factors displacing an atomic beam resonance is the Doppler effect. A beam is formed by effusion of atoms from a source at temperature T , so that the most probable velocity¹ for an atom in the beam is $(3/2)^{1/2} \alpha = (3k_B T/m)^{1/2}$. The magnitude of α is typically a factor of 10^6 smaller than the speed of light.

A velocity-averaged expression for this shift may be found in the following way. The leading term in the near resonance transition probability¹ for a single atom with velocity v is

$$P_{pq} = \sin^2(2bl/v) \cos^2[(\bar{\omega}_0 - \omega')L/2v]. \quad (\text{III.1})$$

Here ω' is the radiation field angular frequency experienced by the atom and we use the prime to denote that it is not quite the same as the applied frequency ω . A slight modification of the usual Doppler shift expression relates ω' and ω :

$$\omega' = \omega \{ 1 - [v(1-R)/c(1+R)] \sin(\xi) \} / [1 - (v^2/c^2)]^{1/2} \quad (\text{III.2})$$

where $v \sin(\xi)$ is the component of atom velocity directed along the propagation vector of the radiation field, assumed to be a running wave. In the atomic-beam problem, we deal with standing waves. These can be considered to be the sum of two running waves, one of amplitude H , incident on the ends of the U-shaped cavity, and one of amplitude RH , reflected from the cavity ends, with R being the reflection coefficient. A net running wave exists only if $R < 1$, and direct calculation gives the $(1-R)/(1+R)$ factor in the first-order Doppler term. Making use of the smallness of $(1-R)$ and $|\sin \xi|$, as well as $(v/c) \ll 1$, Eq. (III.2) becomes

$$\omega' \cong \omega \{ 1 - [v(1-R)/c(1+R)] \sin(\xi) + (v^2/2c^2) \}. \quad (\text{III.3})$$

⁴ J. Holloway and R. Lacey, *Proceedings of the International Conference on Chronometry, Lausanne* (Swiss Society of Chronometry, Neuchatel, 1964), p. 317.

⁵ R. Beehler, W. Atkinson, L. Heim, and C. Snider, *IRE Trans. Instr. I-11*, 231 (1962).

Using this in the transition probability (III.1) and taking the velocity average, we find

$$\langle P_{pq} \rangle = \frac{1}{4} [U_0(\phi) + \cos(\delta_{\text{eff}}) U_1(\phi, \theta) + \sin(\delta_{\text{eff}}) W_1(\phi, \theta)] + \langle \Delta P_{pq} \rangle. \quad (\text{III.4})$$

The notation of Sec. II is used, with

$$\delta_{\text{eff}} \cong -\bar{\omega}_0 L(1-R) \sin(\xi)/c(1+R), \quad (\text{III.5})$$

and

$$\langle \Delta P_{pq} \rangle \cong \frac{1}{4} [(\bar{\omega}_0 \alpha L \theta / 2c^2) U_0(\phi)]. \quad (\text{III.6})$$

The first-order Doppler term has made a contribution identical to that of a phase difference between the radiation fields, denoted by δ_{eff} , and the second-order Doppler term has made a small correction $\langle \Delta P_{pq} \rangle$ to the near resonance transition probability.

Momentarily neglecting the latter contribution, we have the power-dependent frequency shift due to a first-order Doppler effect given by Fig. 1. At optimum intensity, using (II.9) and (III.5), we have

$$\omega_{\text{res}} - \bar{\omega}_0 \cong \bar{\omega}_0 \alpha (1-R) \sin(\xi)/c(1+R). \quad (\text{III.7})$$

The $\sin(\xi) \cong \xi$ factor is to be interpreted as a "representative" value for the beam, with ξ being evidently the angle between a line normal to the line of sight between source and detector (in the plane of the U-shaped cavity), and a line parallel to the waveguide forming the cavity ends. By displacing the source and detector relative to each other along the beam height, thereby varying ξ , the presence of a first-order Doppler shift can be determined.

To develop an expression for the second-order Doppler shift, we can take $\delta_{\text{eff}} = 0$ for simplicity and use an analytical expansion⁶ of $I(\theta)$ for $\theta \ll 1$:

$$I(\theta) \cong \frac{1}{2} (1 - \frac{1}{2} \theta^2).$$

The transition probability for angular frequencies very near $\bar{\omega}_0$ is then

$$\langle P_{pq} \rangle \cong \frac{1}{4} \{ 2 - 4I(\phi) - \frac{1}{2} \theta^2 + (\bar{\omega}_0 \alpha L \theta / 2c^2) [1 - 2I(\phi)] - \theta^2 [d^2 I(\phi) / d\phi^2] \}.$$

The maximum occurs for

$$\theta_{\text{res}} = [L(\bar{\omega}_0 - \omega_{\text{res}}) / \alpha] = (\bar{\omega}_0 \alpha L / 2c^2) \times [1 - 2I(\phi)] / \{ 1 + 2[d^2 I(\phi) / d\phi^2] \}.$$

The power dependence of the resonance frequency is given in Fig. 5. At optimum intensity ($\phi = \phi_0$) the second-order Doppler shift is

$$\omega_{\text{res}} - \bar{\omega}_0 = - (1.24) (\alpha^2 / 2c^2) \bar{\omega}_0. \quad (\text{III.8})$$

Up to now the assumption of a two-level quantum system has been employed. When account is taken of

⁶ N. Kruse and N. Ramsey, J. Math. Phys. **30**, 40 (1951).

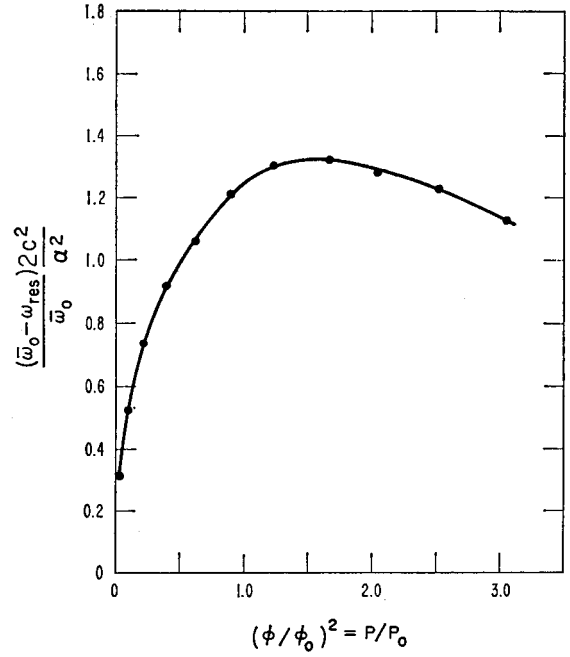


FIG. 5. Theoretical frequency shift due to second-order Doppler effect, as a function of excitation intensity.

neighboring energy levels to the pair involved in a given transition, it is found that an intrinsic shift of the resonance away from the Bohr value results. In general, the magnitude of this "natural" shift is a function of the polarization of the radiation field with respect to the static c field. Such shifts have received attention from several authors,^{3,7} and their details with regard to atomic-beam experiments have been examined elsewhere.⁸ Here we will merely write down the lowest order shift expressions appropriate to the transitions in cesium to be described in Sec. IV.

For the magnetic-field-insensitive transition $(F, M_F) = (4, 0) \leftrightarrow (3, 0)$, the shift for separated-fields excitation is derived to be

$$\omega_{\text{res}} - \bar{\omega}_0 = +3b_0^2 \tan^2(\eta) P / L\bar{\omega}_0 P_0, \quad (\text{III.9})$$

where η is the angle between the oscillating radiation field and the c -field, and b_0 is given by (II.8). For the transitions $(F, M_F) = (4, \pm 1) \leftrightarrow (3, \pm 1)$, the predicted shifts are

$$\omega_{\text{res}} - \bar{\omega}_0 = \pm b_0^2 \tan^2(\eta) P / 15L2\pi(7.00) 10^5 H_c P_0. \quad (\text{III.10})$$

Here H_c is in oersteds, and we assume ideal c -field uniformity; otherwise this expression would contain the factor $k(P)$, described in Sec. II.

⁷ H. Salwen, Phys. Rev. **99**, 1274 (1955); J. Winter, Compt. Rend. **241**, 375, 600 (1955); M. Mizushima, Phys. Rev. **133**, A414 (1964); J. Shirley, Phys. Rev. **138**, B979 (1965).

⁸ R. Harrach, National Bureau of Standards Technical Note 346 (1966).

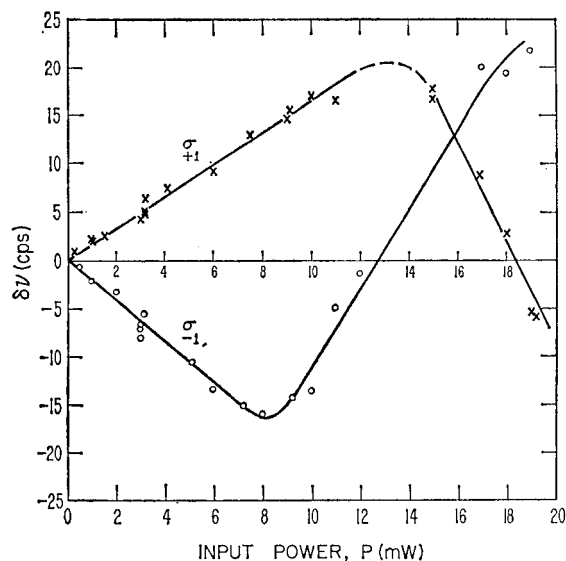


FIG. 6. Power-dependent frequency shifts of the magnetic-field-sensitive transitions σ_{+1} and σ_{-1} of cesium at $\bar{H}_c = 0.0484$ Oe. The shift magnitudes are arbitrarily normalized to be zero at $P=0$.

The properties of the radiation field which we have heretofore neglected are the "anti-rotating" or non-resonant time component of the field, and the electric component. The influence on the resonance frequency of the former was first derived by Bloch and Siegert,⁹ and has since been treated by others.¹⁰ Strictly speaking, the Bloch-Siegert effect is not fundamentally unavoidable, since one could select a radiation field mode in which the magnetic component is rotational rather than oscillatory. In practice this is not convenient or necessary. The leading term of this shift for separated-fields excitation can be shown to be

$$\omega_{\text{res}} - \bar{\omega}_0 = +lb_0^2 P / L\bar{\omega}_0 P_0. \quad (\text{III.11})$$

The electric field component gives a Stark effect, which for cesium was measured by Haun and Zacharias.¹¹ With separated-fields excitation this shift may be written as

$$\omega_{\text{res}} - \bar{\omega}_0 = - (l/L) 2\pi (2.29) 10^{-10} E_0^2 (P/P_0), \quad (\text{III.12})$$

where E_0^2 is the mean square field magnitude (in volts/meter) when the excitation intensity is optimum.

For the specific atomic-beam systems to be studied, we will find in numerically evaluating the frequency shift expressions that the fundamental effects play a decidedly minor role. But in view of current attempts to increase the accuracies of frequency standards into the realm of parts in 10^{14} and beyond, they become of more practical significance.

⁹ F. Bloch and A. Siegert, Phys. Rev. **57**, 522 (1940).

¹⁰ For example, N. Ramsey, Phys. Rev. **100**, 1191 (1955) and J. Shirley, J. Appl. Phys. **34**, 783 (1963).

¹¹ R. Haun, Jr., and J. Zacharias, Phys. Rev. **107**, 107 (1957).

IV. EXPERIMENTS

Interest will be confined to three magnetic dipole σ transitions among the hyperfine-structure levels in the ground state of cesium-133. Using the notation σ_{MF} for the transitions, they are $\sigma_{\pm 1}[(F, M_F) = (4, \pm 1) \leftrightarrow (3, \pm 1)]$ and $\sigma_0[(F, M_F) = (4, 0) \leftrightarrow (3, 0)]$. The dependence of the Bohr frequency of each of these on a weak external magnetic field, H_c , is found from the Breit-Rabi formula¹ to be

$$\begin{aligned} \sigma_{\pm 1}: \nu_0(H_c) &\cong \nu_0(0) \pm (7.000) 10^6 H_c, \\ \sigma_0: \nu_0(H_c) &\cong \nu_0(0) + (426.4) H_c^2, \end{aligned} \quad (\text{IV.1})$$

where H_c is in oersteds, and $\nu_0(0) \cong 9192631770$ cps.

The atomic-beam machine utilized in the first set of experiments to be discussed is a high precision device, referred to as NBS II, which has functioned as a United States frequency standard since 1960. The main features of its components are as follows (and more detailed descriptions are available)¹²: A U-shaped rectangular cavity operated in a $\text{TE}_{1,0,100}$ mode excites the cesium resonance, with the cavity ends separated by a distance $L = 163$ cm. Deflection of the beam is accomplished by two dipolar electromagnets of 4-in.

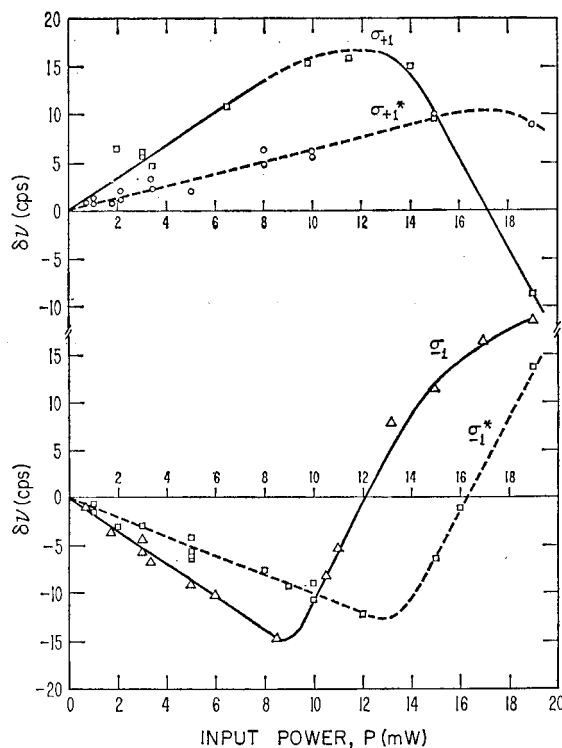


FIG. 7. Power-dependent frequency shifts of the σ_{+1} (upper) and σ_{-1} (lower) resonances for opposite beam directions through the apparatus. An asterisk (*) denotes the reversed beam direction. The data were obtained with $\bar{H}_c = 0.0905$ Oe.

¹² R. Mockler, Advan. Electron. Electron Phys. **15**, 1 (1961); R. Mockler, R. Beehler, and C. Snider, IRE Trans. Instr. **I-9**, 120 (1960).

gap length, which give a field and gradient at the beam of 2100 Oe and 6800 Oe/cm, respectively. An oven containing cesium is maintained at 420°K, resulting in a most probable velocity for cesium atoms in the beam of $(3/2)^{1/2}\alpha = 2.8 \times 10^4$ cm/sec. Detection of the beam is made by a hot (1200°K) wire ribbon of platinum-iridium alloy.

Measurements were made by a servo technique,⁵ using a rubidium gas cell as a reference frequency source. When the excitation intensity was near its optimum value, standard deviations of the measurements on field-sensitive transitions were about 5 parts in 10^{11} for averaging times of a few minutes. For intensities different from the optimum value by a factor of 5 or 6, the statistical fluctuations were larger by an order of magnitude. The speed of data acquisition

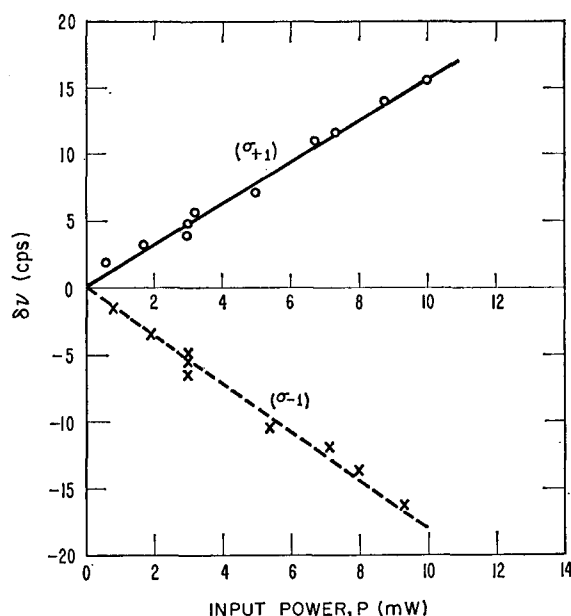


FIG. 8. Example of the highly linear frequency shifts observed for the σ_{+1} and σ_{-1} resonances for input powers below the levels at which the shift directions change sign. For the data shown, $H_c = 0.0283$ Oe.

afforded by the servo-measurement system was essential, since systematic errors due to small, sporadic variations (of order 10^{-5} Oe) in the average c -field magnitude were the limiting error factors when dealing with magnetic field-sensitive transitions. From the relations (IV.1) it is seen that a c -field change of 10^{-5} Oe shifts the frequencies of the $\sigma_{\pm 1}$ resonances by ± 7 cps, or ± 7.6 parts in 10^{10} , while the same variation displaces σ_0 by only 4.6 parts in 10^{14} , at $H_c = 1/20$ Oe.

The power-dependent frequency shifts measured for the $\sigma_{\pm 1}$ transitions are shown in Figs. 6-8, including data at various c -field magnitudes and for both directions of beam traversal. The most notable features of the data are the following. As the intensity of excitation

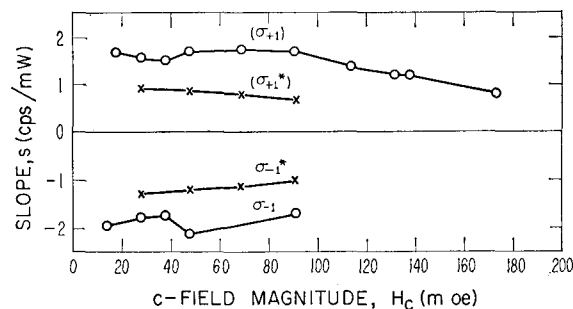


FIG. 9. Summary of data on initial rates of shift, S , in cps/mW, of the σ_{+1} and σ_{-1} resonances, as a function of c -field magnitude and beam direction through the apparatus. An asterisk (*) denotes the reversed beam direction.

is increased from a level well below the optimum value of $P_0 \approx 3.5$ mW, the resonance frequency of σ_{+1} shifts upward linearly at the rate of about 1 part in 10^{10} per milliwatt variation of input power. The precise rate of shift depends on the c -field magnitude and beam direction through the apparatus, as shown in Fig. 9. At an intensity of nearly $4P_0$, a point of slope reversal occurs, and thereafter the resonance frequency begins to decrease with increasing power. The results for the σ_{-1} transition are similar, but with the shift directions reversed. The shifts for the two transitions are not symmetrical, however, with the rate of shift being greater for σ_{-1} and the turn-over point occurring at a lower level of excitation intensity. With the opposite direction of beam traversal, the rates of shift and turn-over point locations are altered by fairly significant amounts.

By contrast, measurements on the σ_0 transition, using the rubidium cell as a reference frequency source, were not sufficiently precise to resolve a power-dependent frequency shift. If any was present, its magnitude was smaller than 2 parts in 10^{12} per milliwatt (see Fig. 10). Subsequently, we will consider more precise results for this transition obtained in an experiment using an atomic-hydrogen maser as a reference.

Attempts to describe the shifts of the field-sensitive resonances in terms of any fundamental effect are completely frustrated, since such descriptions do not fit the data even qualitatively. In particular, by evaluating the shift expressions of Sec. III for the

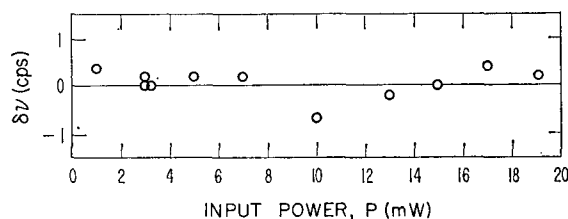


FIG. 10. Absence of a definite power-dependent frequency shift of the σ_0 resonance when Rb gas cell was used as a reference frequency source.

parameters of the NBS II beam machine ($l=1.02$ cm, $L=163$ cm, $\alpha=2.3\times 10^4$ cm/sec), one finds the following predictions for fractional shifts of $\sigma_{\pm 1}$ due to the fundamental effects:

Neighboring levels effect:

$$\Delta\nu/\bar{\nu}_0 \cong \pm (7.2) 10^{-13} [H_c(\text{Oe})]^{-1} \tan^2(\eta) (P/P_0),$$

Bloch-Siegert effect:

$$\Delta\nu/\bar{\nu}_0 \cong + (8.5) 10^{-16} (P/P_0),$$

Stark effect:

$$\Delta\nu/\bar{\nu}_0 \cong - (3.3) 10^{-18} (P/P_0),$$

2nd-order Doppler effect:

$$(\Delta\nu/\bar{\nu}_0)_{P=P_0} = - (3.7) 10^{-13}.$$

Apart from these magnitudes being negligibly small compared to 1 part in 10^{10} , the power dependence and c -field dependence are different from that observed. Also, an experiment to determine a first-order Doppler shift (by varying the angle ξ as discussed in Sec. III) revealed no shift to within a few parts in 10^{12} measurement precision.¹³

The explanation of the observations is found in terms of c -field nonuniformity. The c -field difference factor, $\Delta=4l(\omega_0-\bar{\omega}_0)/\alpha$, was evaluated using calibrated line shape traces of the magnetic dipole σ -transitions among the cesium hfs levels, one of which is shown in Fig. 11. The value for the difference in average c -field magnitudes between the transition and drift regions, $H_c(l)-H_c(L)$, was found to be a function of the particular transition used to determine it. Using the σ_{+1} transition, the result was

$$H_c(l)-H_c(L) = (\nu_0-\bar{\nu}_0)/7.0\times 10^5 \cong +0.0025 \text{ Oe}, \quad (\text{IV.2})$$

while the σ_{-1} transition gave a value smaller by 0.0005 Oe. The reason the values do not agree is that atoms involved in the different transitions sample slightly different spatial regions of the c field. For example, atoms which register the σ_{+1} resonance at the detector are deflected laterally by a force $\mu_{\text{eff}}(\partial H_m/\partial x)$ in the regions of the inhomogeneous magnets, where the effective magnetic dipole moment is $\mu_{\text{eff}} \cong (0.66)$ (Bohr magneton), since $H_m \cong 2000$ Oe.¹² However, atoms which register the σ_{-1} resonance are deflected only half this amount and their trajectories sample a slightly different region of the c field. The Δ -factors for the σ_{+1} and σ_{-1} transitions are then calculated to be +1.95 and -1.56, respectively, and a precise symmetry between the resonance frequency shifts for the two transitions is not to be expected.

A semiquantitative estimate of the shift magnitudes that should result from these c -field difference factors is provided by the curves for $\Delta=1.885$ in Figs. 2 and 4. Using Fig. 2, we would expect the frequency shift magnitude beyond the turn-over point to diminish at a rate given by $[\partial\theta_{\text{res}}/\partial(P/P_0)] = \pm 0.173$, where the \pm sign applies for $\Delta = \pm 1.885$. Making use of Eq. (II.2) with $\alpha/L = 1.41\times 10^2$ (sec)⁻¹ and $P_0 = 3.5$ mW, this is $\partial(\nu_{\text{res}}-\bar{\nu}_0)/\partial P = \mp 1.1$ cps/mW, or ∓ 1.2 parts in 10^{10} per milliwatt. The initial rate of frequency shift, approaching the point of slope reversal, has the opposite sign and is the same order of magnitude, but departs from linearity. Thus the correct order of magnitude and proper signs are predicted for the shifts of the σ_{+1} and σ_{-1} resonance frequencies. However, the experimental curves show highly linear initial shifts (Fig. 8), and the points of slope reversal occur at several times optimum power, while the theoretical turning point occurs a little below optimum power. These disparities between the theoretical and experimental curves are only slightly lessened if it is assumed that the beam experiences excitation by unequal rf amplitudes, so that one of the $\epsilon \neq 0$ curves in Fig. 4 is applicable. The difference in rf amplitudes is determined by the quantity $\cos(2\pi z/\lambda_0)$, as discussed in Sec. II. In the NBS II machine, $0 \leq z \leq 0.48$ cm $\cong (0.1)\lambda_0$, so that the maximum amplitude difference factor expected is $\epsilon \leq 1.25$. The location of the turn-over point occurs below $2P_{\text{opt}}$ for such a factor. The lack of more exact qualitative agreement between the

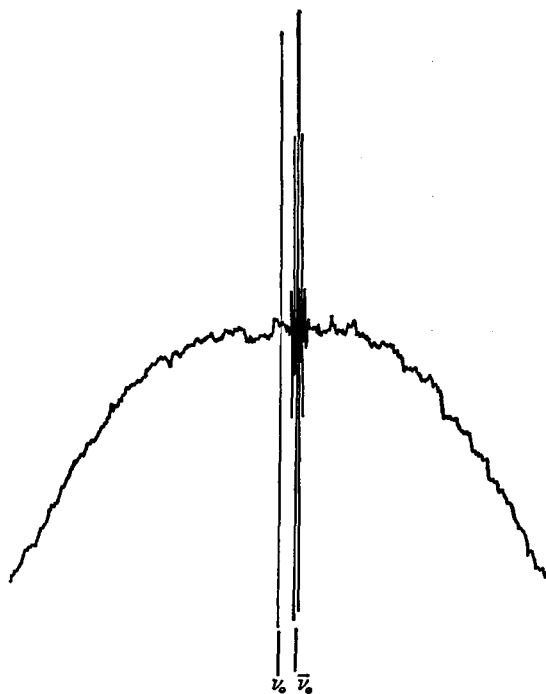


FIG. 11. σ_{-1} resonance line shape, showing pedestal centered at ν_0 and central Ramsey peak at $\bar{\nu}_0$.

¹³ R. Beehler and D. Glaze (private communication).

shapes of the theoretical and experimental curves is likely due to small departures of the actual velocity distribution of atoms from the assumed Maxwellian form.

The adjustment in rates of shift and points of slope reversal that accompanies reversal of the beam direction is primarily a consequence of the Δ -factors not being precisely reproduced in the new alignment. The similar adjustments that occur when the c -field magnitude is varied indicate a small dependence of $[H_c(l) - H_c(L)]$ on the applied c -field value, with the main contribution to this quantity being a result of a residual field in the shielded region.

The fact that any frequency shift of the field-insensitive σ_0 transition was smaller than that of $\sigma_{\pm 1}$ by a factor of 100 or more is explainable by the small value of its Δ -factor. For the σ_0 resonance,

$$\begin{aligned} \omega_0 - \bar{\omega}_0 &= 2\pi(426.4) [\langle H_c^2(l) \rangle - \langle H_c^2(L) \rangle] \\ &\cong 2\pi(426.4) 2\bar{H}_c(l) [\bar{H}_c(l) - \bar{H}_c(L)]. \end{aligned} \quad (IV.3)$$

For a field difference of 0.0025 Oe and $\bar{H}_c(l) = 0.050$ Oe, this equals 0.67 rad/sec, giving $\Delta \cong 1.2 \times 10^{-4}$, and resulting in a fractional frequency shift of about 7×10^{-14} .

Several months after the foregoing experiments were concluded, an opportunity arose to repeat the

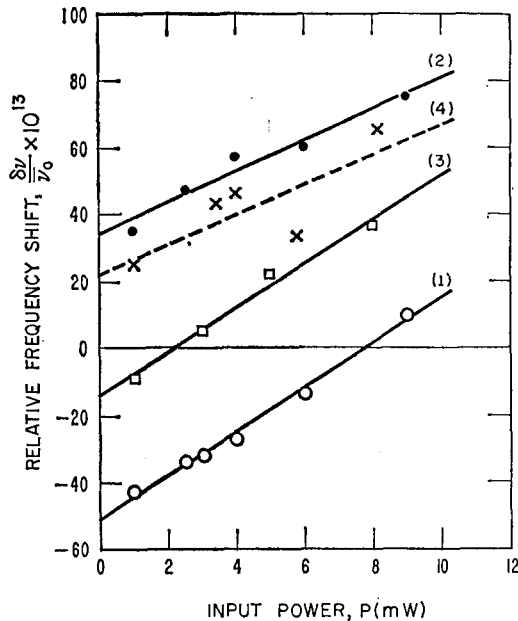


FIG. 12. Power-dependent frequency shifts of the σ_0 transition in the NBS III atomic-beam spectrometer. The least squares determined lines (1) and (3) represent one beam direction, and (2) and (4) the other, in chronological order. The zero point for the frequency shift relative to the H -maser reference is arbitrarily chosen. The data points for lines (1), (2), and (3) are means for $\frac{1}{2}$ -h averaging times, with standard deviations of 2 to 4 parts in 10^{13} . Line (4) was determined in a more brief experiment. The time duration between successive experiments was about 5 days.

power-dependent shift measurements for the σ_0 resonance, using a reference frequency source with much greater precision than was afforded by the rubidium cell. The occasion was an assemblage of various frequency standards for the purpose of intercomparison¹⁴ at the National Bureau of Standards Boulder Laboratories. Among these was a pair of atomic-hydrogen masers from Varian Associates capable of stabilities of a few parts in 10^{13} over a duration of several weeks. With one of these as a reference, the experiments were performed using the atomic-beam machine NBS III, which has served as a frequency standard since 1963. (The atomic beam machine, NBS II, which was used to obtain the earlier data was at this time in the process of being converted to a thallium machine.) For the NBS III device, the drift region length is $L = 366$ cm.

The measured power-dependent frequency shifts are shown in Fig. 12 for three successive reversals of the beam direction through the apparatus. Over the range of excitation intensities considered, the shifts are linear, and data for opposite beam directions show a slightly different slope and a relative frequency offset. The important features of the data are the slopes, zero power (extrapolated) intercepts, and the average values of these quantities for opposite beam directions. These are summarized in Table I.

As in the previous experiments, the interpretation of the results is found in terms of apparatus, rather than fundamental, effects. Cataloging the expected frequency shifts due to the fundamental factors, using $l = 1.02$ cm, $L = 366$ cm, and $\alpha = 2.3 \times 10^4$ cm/sec in the expressions of Sec. III, we have:

Neighboring levels effect:

$$\Delta\nu/\bar{\nu}_0 \cong + (1.1) 10^{-15} \tan^2(\eta) (P/P_0),$$

Bloch-Siegert effect:

$$\Delta\nu/\bar{\nu}_0 \cong + (3.8) 10^{-16} (P/P_0),$$

Stark effect:

$$\Delta\nu/\bar{\nu}_0 \cong - (1.5) 10^{-18} (P/P_0),$$

2nd-order Doppler effect:

$$(\Delta\nu/\bar{\nu}_0)_{P=P_0} = - (3.7) 10^{-13}.$$

The observed shifts are roughly $+3 \times 10^{-12} P/P_0$, with $P_0 \cong 6.0$ mW.

The relative displacement of the resonance for opposite beam directions is attributed to a phase difference between the radiation fields. For a particular beam direction and optimum excitation intensity, phase difference gives an angular frequency shift $\alpha \delta_i/L$, as given by Eq. (II.9). After reversing the beam,

¹⁴ R. Bechler *et al.*, Proc. IEEE (Letter) **54**, 301 (1966).

TABLE I. Summary of experimental results in Fig. 12. The slopes and intercepts, together with their standard deviations, are derived by least-squares analysis.

Experiment	Slope, S (parts in $10^{13}/\text{mW}$)	Avg. slope $\frac{1}{2}(S_i + S_j)$ (parts in $10^{13}/\text{mW}$)	Difference slope $\frac{1}{2}(S_i - S_j)$ (parts in $10^{13}/\text{mW}$)	Zero power intercept (parts in 10^{13})	Avg. zero power intercept (parts in 10^{13})
1	6.58 ± 0.32	5.63 ± 0.33	0.96 ± 0.33	-51.3 ± 1.6	-8.8 ± 1.7
2	4.67 ± 0.58	5.67 ± 0.40	1.00 ± 0.40	$+33.8 \pm 3.0$	$+9.6 \pm 2.0$
3	6.66 ± 0.53	5.58 ± 0.78	1.08 ± 0.78	-14.6 ± 2.7	$+3.9 \pm 4.0$
4	4.49 ± 1.49			$+22.3 \pm 7.5$	

the shift is $\alpha\delta_j/L$, resulting in a frequency difference of $\Delta\nu = \Delta\omega/2\pi = \alpha(\delta_i - \delta_j)/2\pi L$. If $\delta_j = -\delta_i$, the successive beam reversals would give a reproducible frequency difference, $|\Delta\nu| = \alpha|\delta_i|/\pi L$. This was clearly not the case. For either beam direction, the phase difference value was of order 10^{-3} rad, but in reversing the beam direction its precise magnitude was changed. It is felt that this irreproducibility is a consequence of the system being opened to atmospheric pressure in order to interchange the oven and detector.¹⁵ Contaminants in the cavity ends, which can contribute to a phase difference value, then interact with air and moisture, resulting in a modified value. This circumstance could be avoided by designing the system so that it may be kept under vacuum while the oven-detector interchange is made. Both an oven and detector could be situated at each end of the apparatus, with adjustments for positioning the components so that either combination of oven and detector could be used.

The average rate of frequency shift for opposite beam directions, denoted by the subscripts i and j , was reproducible, with the magnitude

$$(S_i + S_j)/2\bar{\nu}_0 \cong +5.6 \times 10^{-13}/\text{mW}. \quad (\text{IV.4})$$

Imbalance between pairs of sidebands in the excitation spectrum provides an interpretation of this result. A spectrum analysis revealed that the brightest sidebands were 44 dB below the primary intensity at ± 60 cps and ± 120 cps away from the primary frequency. Each pair was balanced to within an uncertainty of 2 dB. If the sideband at -60 cps was 1 to 2 dB above that at $+60$ cps, then Eq. (II.14), with $l = 1.02$ cm, $L = 366$ cm, and $P_0 \cong 6.0$ mW, predicts a fractional shift of $+2.0$ to $+4.5$ parts in 10^{13} per milliwatt. Similarly, this imbalance in the ± 120 cps components would give an additional contribution half as large. When the excitation spectrum was changed, by using a different multiplier chain, the rate

of shift was altered by more than a factor of two, confirming the interpretation as a spectrum effect.

The very small beam direction-dependent contribution to the rate of shift,

$$|S_i - S_j|/2\bar{\nu}_0 \cong 1.0 \times 10^{-13}/\text{mW}, \quad (\text{IV.5})$$

is not satisfactorily understood. Phase difference is capable of making such a contribution, as shown, e.g., by the $\delta = 0.005$ -rad curve of Fig. 1, but this has the wrong sign to account for the observations. A possible explanation is found in terms of a first-order Doppler shift due to leakage radiation from the cavity end slots into the drift region, but this has not been convincingly demonstrated.

Supplementary experiments indicated that the power-dependence of the resonance is unaffected by increasing the c -field magnitude above the $1/20$ -Oe operating level, and by reversing the c -field polarity. The displacements in the resonance frequency that accompanied performance of the operations were consistent with expectations based on the quadratic field dependence (IV.1). For example, a residual average field component, $\bar{H}_0(x)$, along the direction of the applied c -field, $\bar{H}_a(x)$, causes the resultant c -field magnitude to change by approximately $2\bar{H}_0(x)$ when the polarity of the applied field is reversed. This shifts the σ_0 resonance frequency by about $(426.4)4\bar{H}_a(x)\bar{H}_0(x)$ cps, and the shift is removed when the applied component is adjusted to restore the net c -field to its original value. From these supplementary experiments we conclude that physical overlap of neighboring resonances, the Millman effect,¹⁶ and the c -field difference quantity, $[H_c(l) - H_c(L)]$, make negligible contributions to a shift of the σ_0 resonance in the NBS III beam machine.

The foregoing analysis suggests that measurements of the radiation-field-dependence of a resonance, under

¹⁵ Another method sometimes used is to rotate the cavity 180° , leaving the oven and detector undisturbed.

¹⁶ See the reference of footnote 1. A consideration of the manner in which the beam samples the $\text{TE}_{1,0,n}$ mode in the NBS machines leads one to expect that the matrix element for the Millman effect is $\delta_i \cong 0$, as discussed in Sec. II of this paper.

varying conditions of beam direction, c -field magnitude, and excitation spectrum, among others, can be a useful tool in evaluating the accuracy of an atomic-beam frequency standard. In the case of a cesium standard, the accurate frequency, $\nu_0(0)$, of the $(F, M_F) = (4, 0) \leftrightarrow (3, 0)$ transition in zero magnetic field, as defined in Eq. (IV.1), can be expressed in terms of measured resonance frequencies at input power P_1 and in a magnetic field \vec{H}_{c1} by an operational equation:

$$\begin{aligned} \nu_0(0) = & \frac{1}{2}[\nu_{\text{res},i}(P_1, \vec{H}_{c1}) + \nu_{\text{res},j}(P_1, \vec{H}_{c1})] \\ & - (426.4)\vec{H}_{c1}^2 - (426.4)(\langle H_{c1}^2 \rangle - \vec{H}_{c1}^2) \\ & - \frac{1}{2}(S_i + S_j)P_1 - \Delta\nu_{\text{Doppler}} - \Delta\nu_H - \dots \quad (\text{IV.6}) \end{aligned}$$

The subscripts i and j refer, as before, to opposite beam directions, and the first term is just the mean frequency for the two directions. The second term corrects to zero magnetic field, and the third term adjusts for the use of \vec{H}_{c1}^2 in the c -field calibration, rather than $\langle H_{c1}^2 \rangle$. The fourth term corrects for effects which give a linear power-dependent shift that vanishes in the limit of zero excitation intensity and is independent of beam direction. (This includes unbalanced sidebands and several of the fundamental effects.) S_i and S_j are experimentally determined slopes (in cps/mW, say) of a linear component of the measured frequency shifts. The fifth term subtracts out the second-order Doppler shift [given by (III.8) if P_1 is the optimum power], and the sixth term takes account for the distortion of the resonance due to inequality in the average c -field magnitudes in the transition and drift regions [see Eqs. (II.10) and (IV.3)]. The relation could be continued to include other contributions¹⁷ which are not treated explicitly here, e.g., physical overlap, cavity pulling, multiplier chain transient phase shifts, and various servo-system effects.

The assessment of accuracy uncertainty is made by considering the uncertainty in each term of Eq. (IV.6). The way that these individual contributions should be combined to arrive at a standard deviation representing the limits of accuracy is described by Beehler *et al.*¹⁷

¹⁷ R. Beehler, R. Mockler, and J. Richardson, *Metrologia* **1**, 114 (1965).

An analysis, using Eq. (IV.6) and the experimental results which have been presented, of the resonance frequency corrections which should be applied to the NBS III atomic-beam frequency standard, together with an itemized account of the uncertainties in the corrections and other contributions to accuracy uncertainty, has been given.¹⁸ The single standard deviation (68% confidence) estimate of inaccuracy for this device is ± 1.1 parts in 10^2 , with the major contribution to inaccuracy coming from the irreproducibility in the measurements of $\nu_{\text{res},i}$ and $\nu_{\text{res},j}$. This source of systematic error is expected to be reduced by installation of the alternate oven-detector system mentioned earlier.

The precisely measured frequency shifts which have been described were shown without exception to arise from imperfections in various features of an atomic-beam apparatus. The frequency shifts generated by the more fundamental effects pale in comparison. There is a disappointing aspect to the description of the apparatus effects, since they depend on parameters that are not precisely known, such as the imbalance between a pair of sidebands or the difference in average magnetic field values sampled by atoms over long spatial regions. Rigorous demonstrations of cause and effect are necessarily replaced by the quest for detailed qualitative and semiquantitative correspondence between theory and the observations. Attributing a result to a given effect is rendered very plausible, but the satisfaction of more exact prediction is missing.

ACKNOWLEDGMENTS

I wish to thank Dr. R. Mockler for suggesting the problem and for his aid and encouragement throughout its solution. For many helpful discussions I am indebted to R. Beehler. The computer program used to evaluate Eq. (II.1) was written by J. Tucker. The experimental results shown in Fig. 12 were obtained by R. Beehler, D. Glaze, and C. Snider.

¹⁸ R. Harrach, *Proceedings of the 20th Annual Frequency Control Symposium, Atlantic City* (U.S. Army Electronics Command, Fort Monmouth, N.J., 1966), p. 424.